

Periodic Tension Disturbance Attenuation in Web Process Lines Using Active Dancers

Prabhakar R. Pagilla*
Associate Professor

Ramamurthy V. Dwivedula
Graduate Student

Yongliang Zhu
Graduate Student

Lokukaluge P. Perera
Graduate Student

School of Mechanical and
Aerospace Engineering
Oklahoma State University,
Stillwater, OK 74078-5016

This paper investigates the role of active dancers in attenuation of web tension disturbances in a web process line. A general structure of the active dancer is considered; governing equations for web spans upstream and downstream to the dancer roller are developed. A structural limitation that facilitates efficient design of the active dancer system for web tension disturbance attenuation is derived and discussed based on the developed model. An open-architecture experimental web platform is developed for conducting real-time control experiments using the active dancer system. The active dancer system model is experimentally identified using the standard system identification techniques available in literature. Three types of control designs were investigated for the active dancer system: a proportional-integral-derivative controller, an internal model based controller, and a linear quadratic optimal controller. Data collected from a series of experiments using the three control designs validate the usefulness of the active dancers in attenuating web tension disturbances in a web process line. A representative sample of the experimental data is presented and discussed. [DOI: 10.1115/1.1590678]

1 Introduction

The term web is used to describe materials that are manufactured and processed in a continuous, flexible strip form. Web materials cover a broad spectrum from extremely thin plastics to paper, textiles, metals, and composites. Web processing pervades almost every industry today. With the need for increased performance and productivity in the web processing industry, accurate modeling and effective controller design for web handling systems are essential for increasing the web processing speed and the quality of the processed web. It is important to maintain web tension within the desired limits under a wide range of dynamic conditions such as speed changes, variations in roll sizes, and web properties. Tension variations affect printing quality and tend to cause web breakage and wrinkles.

A dancer mechanism consists of a web roller which is either connected to a fixed support by passive elements such as springs and dampers or is force loaded in opposition to the web tension. Dancer mechanisms are commonly used to attenuate tension disturbances caused by uneven wound rolls, eccentric rolls, misalignment of idle rollers, and slacks in webs. A dancer mechanism is also used as a feedback element in a number of web tension control systems. The tension control system is driven by the variations in the position of the dancer mechanism as opposed to the variations in actual tension from the desired tension.

Passive dancers can be divided into two categories, namely dancer rollers with passive elements such as springs and dampers and inertia compensated dancer rollers. Passive dancers are known to act as good tension feedback elements and/or tension disturbance attenuators for low speed web lines; they have been known to have limitations in dealing with a wide range of dynamic conditions and to cause resonance problems. In inertia compensated passive dancers, the resonant frequency of the dancer roller is mainly determined by its mass. Thus, to increase the tension disturbance frequency range that can be attenuated, the dancer roller mass must be reduced. However, the weight of the

dancer roller needs to be twice the reference web tension, which limits any changes to the dancer roller mass to increase the resonant frequency. It is expected that introducing an active element into a dancer mechanism gives a control engineer more flexibility in attenuating periodic tension disturbances of a wide range of frequencies and also to lower tension fluctuations. The focus of this paper is on modeling and experimental evaluation of an active dancer system for periodic tension disturbance attenuation.

Early development of mathematical models for longitudinal dynamics of a web can be found in Refs. [1–4]. In Ref. [1], a mathematical model for longitudinal dynamics of a web span between two pairs of pinch rolls, which are driven by two motors, was developed. This model does not predict tension transfer and does not consider tension in the entering span. A modified model that considers tension in the entering span was developed in Ref. [3]. In Ref. [4], the moving web was considered as a moving continuum and general methods of continuum mechanics were used in the development of a mathematical model. The study in Ref. [4] included the steady state and transient behavior of tensile force, stress, and strain in a web as functions of variables such as wrap angle, position and speed of the driven rolls, density, cross-sectional area, modulus of elasticity, and temperature.

In [5], equations describing web tension dynamics are derived based on the fundamentals of web behavior and the dynamics of the drives used for web transport; an example system was considered to compare torque control versus velocity control of a roll for regulation of tension in a web. Nonideal effects such as temperature and moisture change on web tension were studied in Ref. [6]; based on the models developed, methods for distributed control of tension in multispan web transport systems were studied; analysis of a multispan web system with a passive dancer for minimizing disturbances due to eccentric unwind roll was also given. An overview of lateral and longitudinal dynamic behavior and control of moving webs was presented in Ref. [7]. A review of the problems in tension control of webs can be found in Ref. [8].

Discussions on tension control versus strain control and torque control versus velocity control were given in Ref. [9]; modeling and design of a tension control station with both inertia compensated dancers and classical passive dancers were also given. A study on dynamic behavior of passive dancers in web transport systems was reported in Ref. [10]. Computer simulation studies were conducted on an example system to investigate disturbance

*Corresponding e-mail address: pagilla@ceat.okstate.edu

Contributed by the Dynamic Systems, Measurement, and Control Division of THE AMERICAN SOCIETY OF MECHANICAL ENGINEERS for publication in the ASME JOURNAL OF DYNAMIC SYSTEMS, MEASUREMENT, AND CONTROL. Manuscript received by the ASME Dynamic Systems and Control Division September 25, 2001; final revision, January 21, 2003. Associate Editor: C. Rahn.

rejection for three cases: (1) without a dancer; (2) with a classical dancer with passive elements; and (3) with an inertia compensated dancer. Based on the simulation results it was concluded that better attenuation of tension disturbances in a web line can be achieved with a dancer as opposed to a web line without a dancer.

An active dancer system for reducing tension variations in wire and sheet materials was proposed in Ref. [11]. Experimental results were reported based on an apparatus consisting of a stationary web around a dancer roller. The main drawback of the apparatus is that the results can be obtained only for a stationary web. Construction of an active dancer system that is capable of rejecting cyclic process induced tension disturbances was reported in Ref. [12]; the main drawback in this work is that a first-order model for the span tension dynamics is used, which does not reflect the tension behavior of the spans upstream/downstream of the dancers.

In this paper, span tension dynamics for upstream and downstream spans of the active dancer roller are developed; a typical active dancer system is considered and the governing equations are derived. An experimental web platform has been developed to investigate the usefulness of the active dancer system for tension disturbance attenuation. Three types of control designs, i.e., proportional-derivative-integral control, internal model control, and linear quadratic optimal control, were experimentally investigated for the active dancer system. Experimental results show that considerable periodic tension disturbance attenuation is possible using an active dancer system. Further, analysis of the active dancer system model gives a structural limitation on its design; the length of the downstream span of the dancer roller must be smaller than the upstream span for efficient tension disturbance attenuation using an active dancer. A numerical example is given to illustrate this limitation.

The contributions of this work over prior work reported in literature are: (1) development of a dynamic model of web tension for spans upstream and downstream to the dancer roller, (2) development of an experimental web platform containing an active dancer system and validation of the model developed via experiments on this platform, (3) discussion of issues related to the design limitations of the active dancer system, and (4) experimental evaluation of three well-known controllers for attenuation of tension disturbances.

The remainder of the paper is organized as follows. Section 2 develops the mathematical model for web spans upstream and downstream to the dancer roller and presents a linearized set of equations for the developed model. Section 3 considers a general configuration of the active dancer system and presents an input-output model. In Sec. 4, some considerations on the design of the active dancer system are presented and discussed. The experimental web platform used for real-time control experiments using the active dancer system is described in Sec. 5. Identification of the active dancer system is given in Sec. 6. Details of the three implemented controllers and results of the experiments are discussed in Sec. 7. Conclusions of the paper and some future work are given in Sec. 8. A list of symbols used in the paper is also given.

2 Tension Dynamics of Web Spans Next to the Active Dancer Roller

It is well known in the web handling literature [4,13] that the tension dynamics of a general web span shown in Fig. 1 is given by

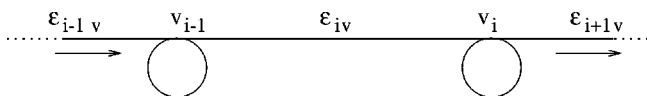


Fig. 1 General web span

$$L_i \frac{d}{d\tau} \epsilon_{iv} = v_i - v_i \epsilon_{iv} - v_{i-1} + v_{i-1} \epsilon_{(i-1)v}, \quad (1)$$

where ϵ_{iv} denotes the strain in the i th web span due to velocity variations. Throughout the paper it is assumed that the i th span precedes the i th roller. In dancer systems, the strain in web spans adjacent to the dancer roller is due to web velocity variations and the dancer roller translational movement. In this section, the tension dynamics in web spans upstream and downstream to the dancer roller are derived by noting that the net strain is equal to the sum of the strains due to the web velocity variation and the strain due to dancer movement.

A general dancer subsystem as shown in Fig. 2 is considered in deriving expressions for strain in the upstream and downstream spans due to the movement of the dancer roller. In Fig. 2, the solid lines represent initial position of the dancer roller and the dashed lines represent the position of the dancer when it moves by a distance of x , that is, $EE_1 = x$.

To derive the strain in the upstream span, note that the initial length of the upstream span is L_1 and the length of the span when the dancer roll moves by a distance of x is $L_1 + \delta L_1 = AF_1$. Notice that

$$L_1 + \delta L_1 = AF_1 = AG_1 - F_1G_1. \quad (2)$$

From the triangle ABG_1 , $AG_1 = BG_1 / \sin(\theta_1 + \delta\theta_1)$ and from the triangle $E_1F_1G_1$, $F_1G_1 = E_1F_1 \tan(\theta_1 + \delta\theta_1) = r \tan(\theta_1 + \delta\theta_1)$. Thus, Eq. (2) can be simplified to

$$\begin{aligned} L_1 + \delta L_1 &= \frac{BG_1}{\sin(\theta_1 + \delta\theta_1)} - r \tan(\theta_1 + \delta\theta_1) = \frac{BE + EE_1 + E_1G_1}{\sin(\theta_1 + \delta\theta_1)} \\ &\quad - r \tan(\theta_1 + \delta\theta_1) = \frac{BG - EG + EE_1 + E_1G_1}{\sin(\theta_1 + \delta\theta_1)} \\ &\quad - r \tan(\theta_1 + \delta\theta_1). \end{aligned} \quad (3)$$

Further notice that from the triangles ABG , EFG , and $E_1F_1G_1$, the following relationships can be obtained: $BG = AG \sin \theta_1 = (AF + FG) \sin \theta_1 = (L_1 + r \tan \theta_1) \sin \theta_1$, $EG = r / \cos \theta_1$, and $E_1G_1 = r / \cos(\theta_1 + \delta\theta_1)$. Thus,

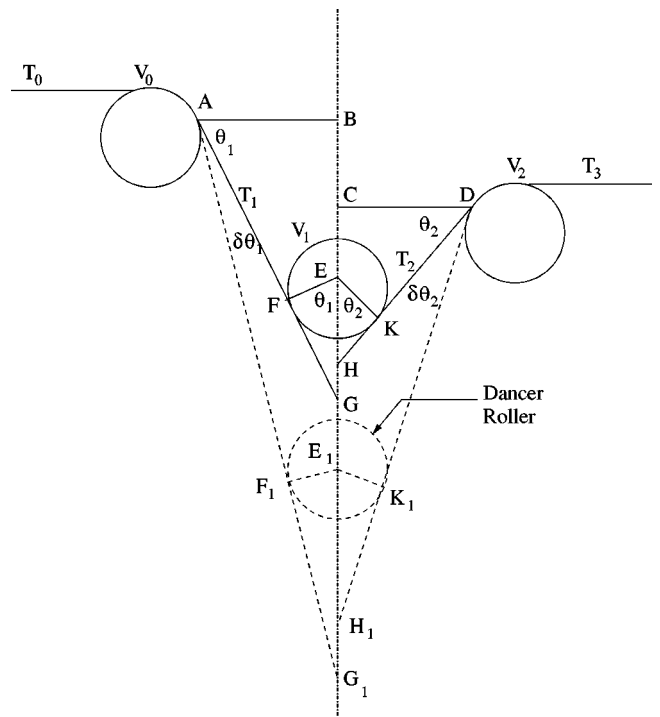


Fig. 2 Dancer spans: unstretched and stretched conditions

$$L_1 + \delta L_1 = \frac{(L_1 + r \tan \theta_1) \sin \theta_1 - \frac{r}{\cos \theta_1} + x + \frac{r}{\cos(\theta_1 + \delta \theta_1)}}{\sin(\theta_1 + \delta \theta_1)} - r \tan(\theta_1 + \delta \theta_1). \quad (4)$$

Typically, the displacement of the dancer roller is much smaller than the length of the web span. It can be assumed that the angle $\delta \theta_1$ is very small, i.e., $\cos \delta \theta_1 \approx 1$ and $\sin \delta \theta_1 \approx 0$. With this assumption, Eq. (4) reduces to

$$L_1 + \delta L_1 \approx L_1 + \frac{x}{\sin \theta_1}.$$

Therefore, the strain induced in the upstream web span due to the movement of the dancer roller is given by

$$\varepsilon_{1d} = \frac{\delta L_1}{L_1} \approx \frac{x}{L_1 \sin \theta_1}. \quad (5)$$

By a similar argument, the strain induced in the downstream span is

$$\varepsilon_{2d} = \frac{\delta L_2}{L_2} \approx \frac{x}{L_2 \sin \theta_2}. \quad (6)$$

Noting that the strain in the upstream span is sum of the strains due to web velocity variations and the dancer displacement, i.e., $\varepsilon_1 = \varepsilon_{1v} + \varepsilon_{1d}$, we can write

$$L_1 \frac{d}{d\tau} \varepsilon_1 = L_1 \frac{d}{d\tau} \varepsilon_{1v} + L_1 \frac{d}{d\tau} \varepsilon_{1d}. \quad (7)$$

Substituting Eqs. (1) and (5) into Eq. (7) results in

$$L_1 \frac{d}{d\tau} \varepsilon_1 = v_1 - v_1 \varepsilon_{1v} - v_0 + v_0 \varepsilon_{ov} + \frac{\dot{x}}{\sin \theta_1}.$$

Under the assumption that the web is elastic, i.e., $\varepsilon_i = t_i / EA$, we obtain

$$L_1 \dot{t}_1 = EA(v_1 - v_0) + (v_0 t_0 - v_1 t_1) + \frac{EA v_1}{L_1} \frac{x}{\sin \theta_1} + EA \frac{\dot{x}}{\sin \theta_1}. \quad (8)$$

For the downstream span, the total strain is the sum of the strains due to web velocity variations and the dancer motion, i.e., $\varepsilon_2 = \varepsilon_{2v} + \varepsilon_{2d}$, which gives

$$L_2 \frac{d}{d\tau} \varepsilon_2 = L_2 \frac{d}{d\tau} \varepsilon_{2v} + L_2 \frac{d}{d\tau} \varepsilon_{2d}. \quad (9)$$

Using Eqs. (1) and (6), Eq. (9) can be written as

$$L_2 \frac{d}{d\tau} \varepsilon_2 = v_2 - v_2 \varepsilon_{2v} - v_1 + v_1 \varepsilon_{1v} + \frac{\dot{x}}{\sin \theta_2}. \quad (10)$$

Equation (10) can be further simplified by noting that $\varepsilon_{1v} = \varepsilon_1 - \varepsilon_{1d}$, $\varepsilon_{2v} = \varepsilon_2 - \varepsilon_{2d}$, $\varepsilon_1 = t_1 / EA$, and $\varepsilon_2 = t_2 / EA$, to obtain

$$L_2 \dot{t}_2 = EA(v_2 - v_1) + (v_1 t_1 - v_2 t_2) + \left(\frac{v_2}{L_2 \sin \theta_2} - \frac{v_1}{L_1 \sin \theta_1} \right) EA x + EA \frac{\dot{x}}{\sin \theta_2}. \quad (11)$$

Equations (8) and (11) are nonlinear involving cross-product terms such as $v_i t_i$. To obtain linearized equations around given reference values of web velocity (v_r), web tension (t_r), and dancer displacement ($x_r = 0$), let $V_i = v_i - v_r$, $T_i = t_i - t_r$, and $X = x$ represent the deviations. Substituting into Eqs. (8) and (11), we obtain the linearized dynamics of web spans upstream and downstream to the dancer roller as

$$L_1 \dot{T}_1 = (EA - t_r)(V_1 - V_0) + v_r(T_0 - T_1) + \frac{EA}{L_1 \sin \theta_1} v_r X + \frac{EA \dot{X}}{\sin \theta_1}, \quad (12)$$

$$L_2 \dot{T}_2 = (EA - t_r)(V_2 - V_1) + v_r(T_1 - T_2) + EA v_r \left(\frac{1}{L_2 \sin \theta_2} - \frac{1}{L_1 \sin \theta_1} \right) X + \frac{EA \dot{X}}{\sin \theta_2}. \quad (13)$$

3 Active Dancer System

The web span dynamics developed in the previous section was for a general case of a dancer roller which is not uniform with respect to the adjacent rollers. It is convenient to measure the tension in the spans if the dancer roller is centrally located between the upstream and downstream rollers and the wrap angle on the dancer roller is 180 deg, i.e., $\theta_1 = \theta_2 = 90$ deg. Further, the angle of wrap remains the same for the unstretched and stretched conditions of the web spans; therefore the tension dynamics is not nonlinear in terms of the angle of wrap on the dancer roll. With this observation, an active dancer system as shown in Fig. 3 is considered. This system contains web spans adjacent to the dancer roller in the upstream and downstream directions and three rollers including the dancer roller. All the variables shown in Fig. 3 represent variations from their reference values. It is assumed that T_0 is the upstream tension disturbance that needs to be rejected using the active dancer.

The angular dynamics of each roller is given by

$$J_i \dot{\omega}_i = -B_{f_i} \omega_i + R_i(t_{i+1} - t_i), \quad (14)$$

where $i = 0, 1, 2$. Assuming that there is no slip on the rollers, the web velocity on each roller is $v_i = R_i \omega_i$. Therefore, the linearized dynamics of web velocity on each roller is given by

$$J_i \dot{V}_i = -B_{f_i} V_i + R_i^2(T_{i+1} - T_i). \quad (15)$$

Using $\theta_1 = \theta_2 = 90$ deg in Eqs. (12) and (13) and assuming that the three rollers are identical, i.e., $J_i = J$ and $R_i = R$, the dynamic equations for the active dancer system shown in Fig. 3 are

$$\beta \dot{V}_0 = -\gamma V_0 + (T_1 - T_0), \quad (16)$$

$$\tau_1 \dot{T}_1 = -T_1 + T_0 + \alpha(V_1 - V_0) + \frac{\alpha}{\tau_1} X + \alpha U, \quad (17)$$

$$\beta \dot{V}_1 = -\gamma V_1 + (T_2 - T_1), \quad (18)$$

$$\tau_2 \dot{T}_2 = -T_2 + T_1 + \alpha(V_2 - V_1) + \alpha \left(\frac{1}{\tau_2} - \frac{1}{\tau_1} \right) X + \alpha U, \quad (19)$$

$$\beta \dot{V}_2 = -\gamma V_2 + (T_3 - T_2), \quad (20)$$

$$\dot{X} = U, \quad (21)$$

where $\beta = J/R^2$, $\gamma = B_f/R^2$, $\alpha = EA/v_r$, $\tau_1 = L_1/v_r$, and $\tau_2 = L_2/v_r$.

Since the value of EA is much larger than t_r for most webs, the t_r term is neglected in obtaining Eqs. (17) and (19) from Eqs. (12) and (13).

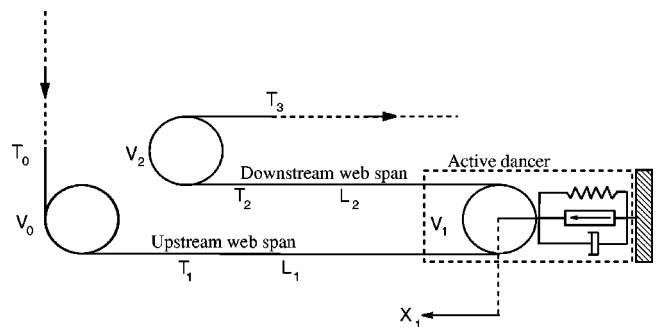


Fig. 3 Active dancer system

4 Design Considerations

Combining Eqs. (16)–(21), the input-output dynamic model [14] for the active dancer system is

$$T_2(s) = \frac{D_{ad}(s)}{C_{ad}(s)}U(s) + \frac{A_{ad}(s)}{C_{ad}(s)}T_0(s) + \frac{B_{ad}(s)}{C_{ad}(s)}T_3(s), \quad (22)$$

where the input $U(s)$ is the dancer translational velocity, and

$$A_{ad}(s) = (\eta s + 1)^2,$$

$$B_{ad}(s) = [\eta s(\tau_1 s + 1) + 2],$$

$$C_{ad}(s) = \{[\eta s(\tau_1 s + 1) + 2][\eta s(\tau_2 s + 1) + 2] - (\eta s + 1)\},$$

$$D_{ad}(s) = \beta \left[(\eta s + 1) \left(s + \frac{1}{\tau_1} \right) + [\eta s(\tau_1 s + 1) + 2] \left(s + \frac{1}{\tau_2} - \frac{1}{\tau_1} \right) \right],$$

where $\eta = Jv_r/EAR^2$. The input/output model has been obtained by assuming that the roller bearing friction is negligible. A full expression with nonzero bearing friction can be found in Ref. [14]. Also, notice that the model is obtained under the assumption that the moment of inertia and radius of all the rollers in the dancer system are the same, i.e., $J_i = J$ and $R_i = R$ for $i = 0, 1, 2$.

Expansion of the numerator, $D_{ad}(s)$, and the denominator, $C_{ad}(s)$, of the plant transfer function gives

$$C_{ad} = \eta^2 \tau_1 \tau_2 s^4 + \eta^2 (\tau_1 + \tau_2) s^3 + \eta (\eta + 2\tau_1 + 2\tau_2) s^2 + 3\eta s + 3 \quad (23)$$

$$D_{ad} = \beta \eta \tau_1 s^3 + \beta \eta \left(1 + \frac{\tau_1}{\tau_2} \right) s^2 + \beta \left(3 + \frac{\eta}{\tau_2} \right) s + \beta \left(\frac{2}{\tau_2} - \frac{1}{\tau_1} \right). \quad (24)$$

Notice that, if $\tau_2 > 2\tau_1$, i.e., $L_2 > 2L_1$, then the constant term of the numerator polynomial, $D_{ad}(s)$, is negative, which results in a right-half-plane zero.

It is common knowledge from classical root-locus analysis that as the feedback gain increases, the closed-loop poles migrate to the positions of the open-loop zeros. Since the active dancer system has a right-half-plane zero, high-gain instability will result. Further, it is also well known that a right-half-plane zero, particularly that is on the real axis and close to zero, can cause severe bandwidth limitations [15]. Therefore, for efficient tension disturbance attenuation using an active dancer, it is necessary to construct the active dancer system such that the downstream span length is smaller than the upstream span length.

To illustrate the effect of the open-loop zero, root-locus plot is employed for various span lengths. Other physical properties of the web and rollers are kept constant, which are exactly same as the ones used in the experiments. The closed-loop characteristic equation with proportional feedback control, i.e., $U(s) = -K_p T_2(s)$, is

$$1 + K_p \frac{D_{ad}(s)}{C_{ad}(s)} = 0, \quad (25)$$

where K_p is the proportional gain.

Figure 4 shows the root-locus plot and the location of the open-loop poles and zeros for $L_1 = 0.9144$ m (36 in.) and $L_2 = 0.2286$ m (9 in.). Figure 4 shows that the proportional gain K_p can be chosen as large as possible. Thus, the disturbance effect on the span downstream to the dancer roll can be attenuated by an arbitrary amount by the choice of K_p . Notice that after a certain value any increase in K_p results in moving a pair of closed-loop poles towards the imaginary axis. Hence, appropriate choice of the gain K_p must be made such that the closed-loop poles are far away from the imaginary axis.

Figure 5 shows the root-locus plot and the location of the open-loop poles and zeros for $L_1 = L_2 = 0.2286$ m (9 in.). In this case, there is a pair of complex-conjugate open-loop poles very close to a pair of complex-conjugate zeros. Thus, any choice of the gain cannot move this pair of open-loop poles further to the left-half-

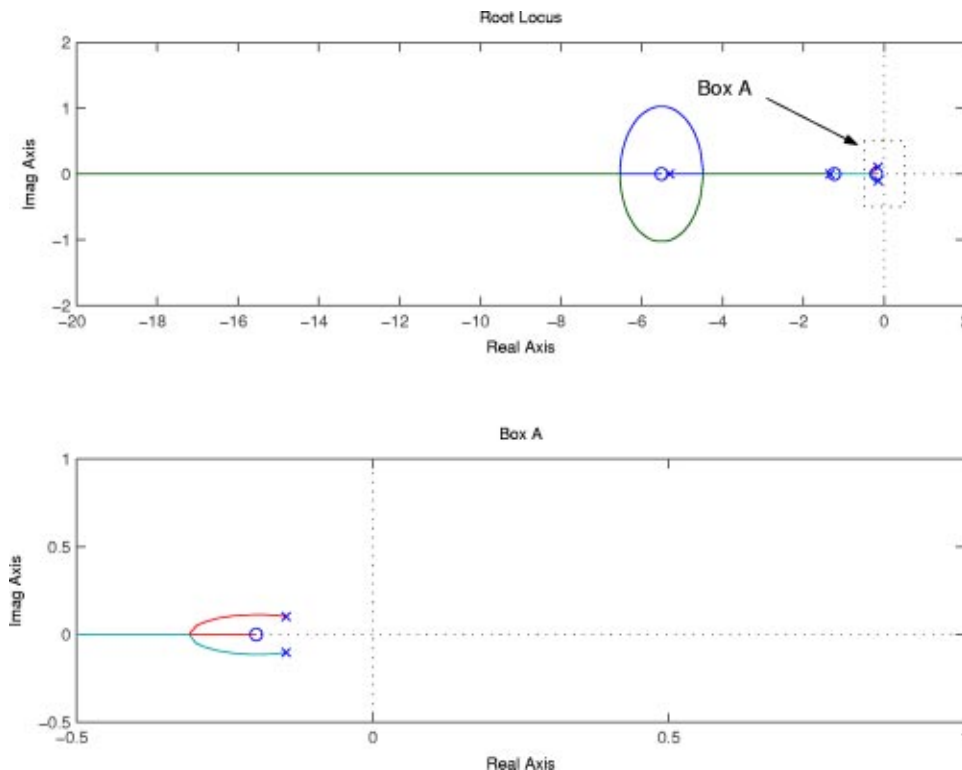


Fig. 4 Root locus plot for $L_1 > L_2$

plane away from the imaginary axis. The effectiveness of the active dancer to attenuate tension disturbances is reduced.

The root-locus plot and location of open-loop poles and zeros for $L_1=0.2286$ m (9 in.) and $L_2=0.9144$ m (36 in.) is shown in Fig. 6. In this case, the root-locus crosses the imaginary axis and enters the right-half plane when K_p exceeds a certain value. For

the numerical example considered, as shown in Fig. 6, a branch of the root locus moves to the right-half plane for a very small value of K_p .

Root-locus plots obtained by varying β and η did not show any appreciable change in the form of the root locus. In all these cases, a small value of K_p rendered the closed-loop system unstable for

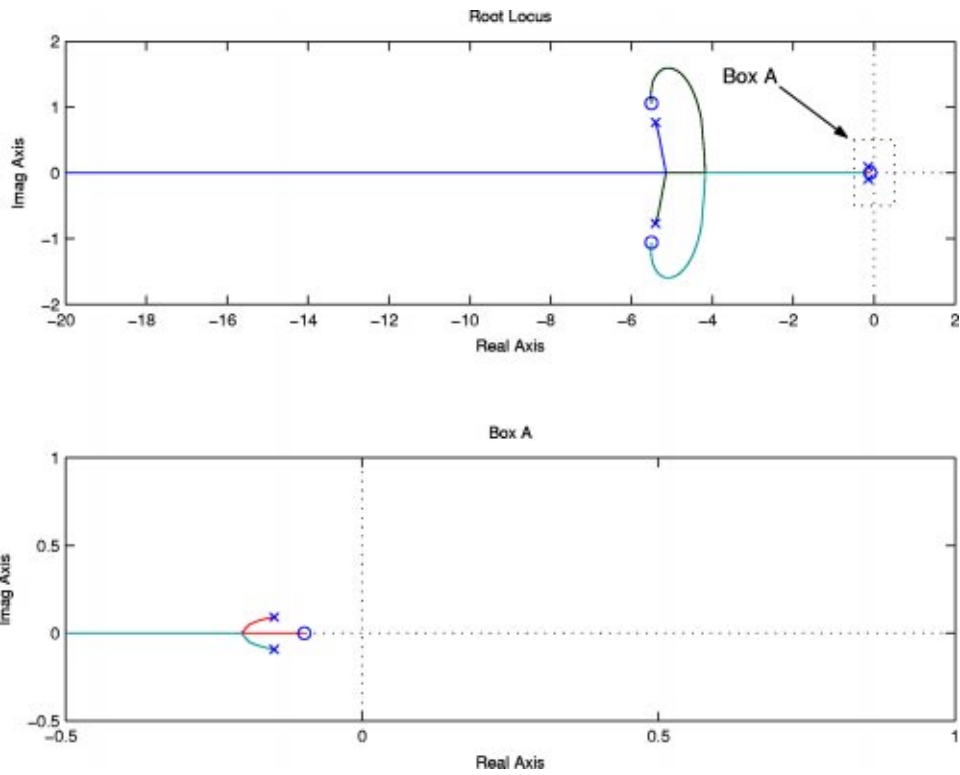


Fig. 5 Root locus plot for $L_1=L_2$

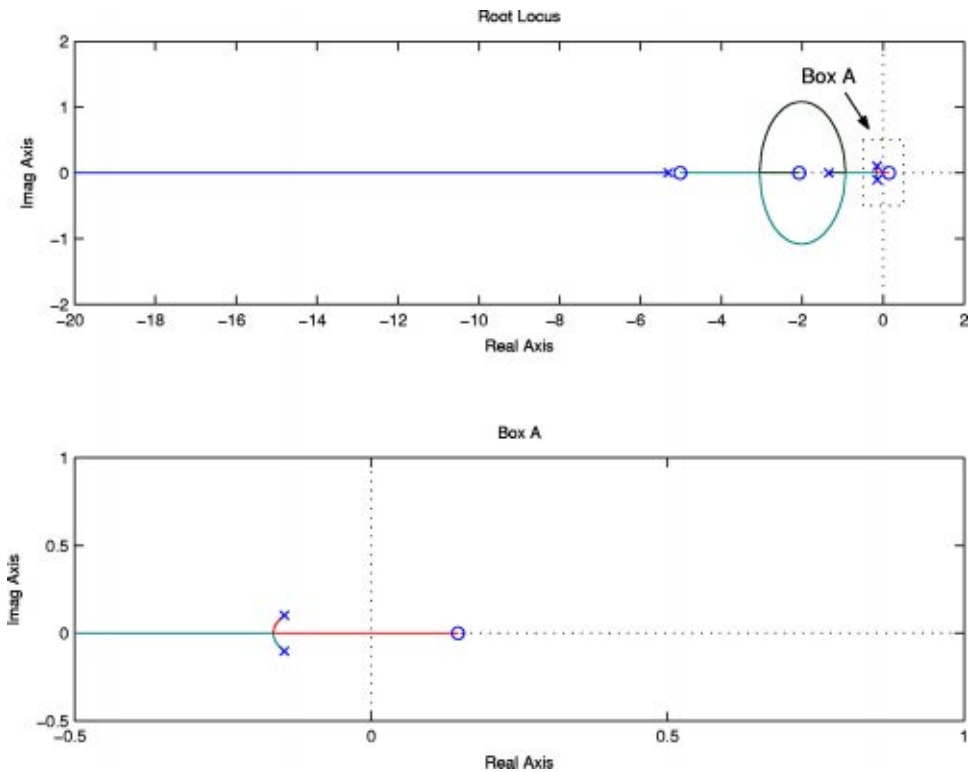


Fig. 6 Root locus plot for $L_1 < L_2/2$

the case of $L_2 > 2L_1$. Notice that variations of β and η in the input-output model reflect variations of web and roller properties, E, A, J, R, B_f , etc.

An intuitive explanation of the effect of span length is given in the following. Assuming that the web is mostly elastic, it is common practice in the web handling community to model a web span as an elastic spring with a spring constant $K_n = E_n A_n / L_n$. The spring constants of the upstream and the downstream web spans to the dancer roller are $K_1 = EA/L_1$ and $K_2 = EA/L_2$, respectively, as shown in Fig. 7.

If $L_1 \geq L_2$, $K_1 \leq K_2$, then any motion of the dancer roller results in larger tension variations in span 2 than in span 1. Thus, rejection of periodic disturbances from the spans upstream of the dancer roller into the spans downstream of the dancer roller is possible in this case. If $L_1 < L_2/2$, $K_1 > 2K_2$, then periodic dancer motion induces larger tension disturbances into the upstream span than it rejects in the downstream span due to feedback of tension T_2 .

5 Experimental Web Platform

A sketch of the open-architecture experimental web platform together with an active dancer system is shown in Fig. 8. Pictures of the complete experimental platform and the active dancer system are shown in Figs. 9 and 10, respectively. In the active dancer system, shown in Fig. 10, the bottom most roller is the active dancer roller. The web platform mainly consists of an endless web line with a number of rollers, an active dancer system, web guides for maintaining lateral position. The term endless web line refers to a web line without unwind and rewind rolls. This type of platform mimics most of the features of a process section of a web processing line.

Mechanical components used in the platform include 16 idle rollers, a master speed roller with a nip roller, an electric motor, and a passive dancer system with a pneumatic cylinder. The width of each roller is 0.2032 m (8 in.) and the diameter is 0.127 m (5 in.), except for the master speed roller, which has a diameter of 0.254 m (10 in.). A nip roller on the master speed roller is used to reduce slip during startup. The master speed roller sets the desired transport velocity of the web. Air pressure in the pneumatic cylinder of the passive dancer roll is used to set the desired reference web tension. The active dancer system consists of an electromechanical actuator, a guide way with the dancer roller mounted on it, and load cells on the idle roller downstream of the dancer roller. A Pentium 450-MHz computer with a Keithley DAS 1601 digital

data acquisition board is used for real-time control experiments. A control sampling period of 5 ms is used in all the experiments.

The measured signals on the experimental web platform (see sketch in Fig. 8) include the velocity of the web measured at the roller immediately downstream of the master speed roller, tension from both load cells shown in Fig. 8, translational velocity of the dancer roller, and lateral position of the web downstream of the guide system. These signals are used during system identification, control, and monitoring.

A transparent polyester film is used as the web material, which has the following properties: $E = 4.136 \times 10^9 \text{ N/m}^2$ ($6 \times 10^5 \text{ PSI}$), $A = 0.0819 \text{ m}^2$ ($1.27 \times 10^{-4} \text{ in.}^2$), $J = 0.0282 \text{ kg m}^2$ (96.21 lb in.^2), and $R = 63.5 \text{ mm}$ (2.5 in.). The length of the web spans upstream and downstream to the dancer roller are 36 and 9 in., respectively.

Periodic tension disturbances upstream of the dancer roller are created by introducing an out-of-round roll surface into an idle roller in the web line as shown in Fig. 8. Load cells that are mounted on the roller immediately downstream of the out-of-round idle roller measure the amount of tension disturbance that is being generated. The fundamental frequency of the periodic tension disturbance for a given out-of-round roller surface increases with increase in web speed.

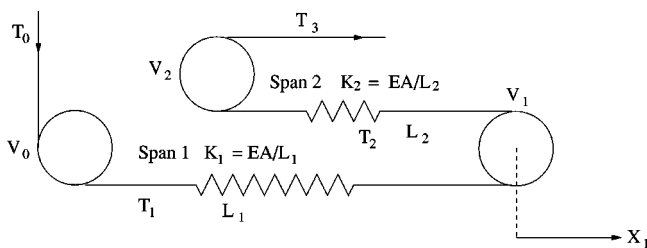


Fig. 7 Interpretation of the effect of span lengths

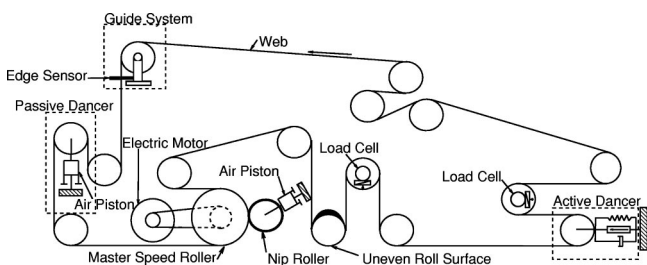


Fig. 8 Sketch of the experimental web platform

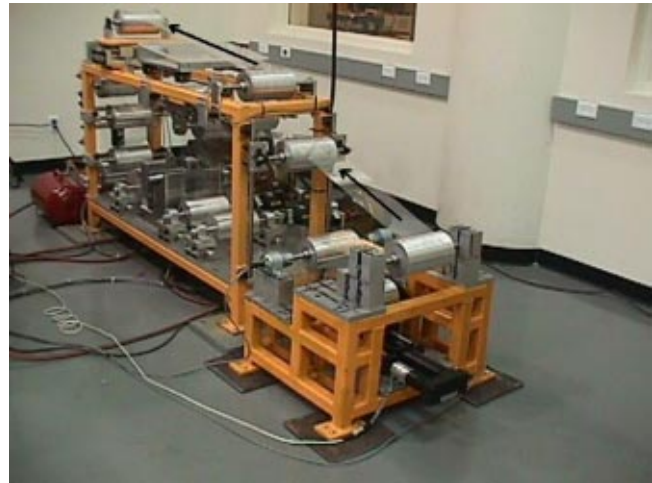


Fig. 9 Picture of the web platform

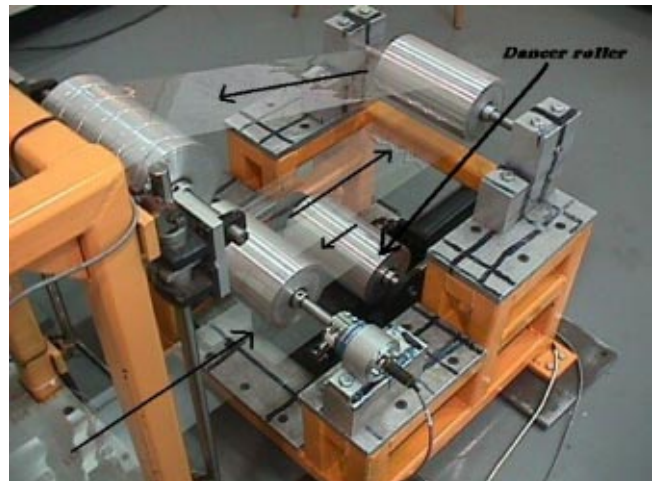


Fig. 10 Picture of the active dancer system

6 System Identification

The transfer function $[T_2(z)/U(z)]$ from the dancer velocity to the tension in the span downstream to the dancer roller is considered for identification. The discrete-time equivalent of the continuous-time input-output model, Eq. (22), with a sampling period of 5 ms, is

$$T_2(z) = 10^{-2} \frac{4.233z^3 - 12.55z^2 + 12.41z - 4.089}{z^4 - 3.966z^3 + 5.897z^2 - 3.897z + 0.9659} U(z) + 10^{-5} \frac{9.537z^3 - 9.635z^2 - 9.324z + 9.421}{z^4 - 3.966z^3 + 5.897z^2 - 3.897z + 0.9659} T_0(z) + 10^{-6} \frac{6.812z^3 - 6.828z^2 - 6.687z + 6.702}{z^4 - 3.966z^3 + 5.897z^2 - 3.897z + 0.9659} T_3(z). \quad (26)$$

In the above conversion, we have used the same numerical values for parameters as given in Sec. 5 with a reference web velocity of 1.266 m/s (250 FPM). To experimentally identify the transfer function $[T_2(z)/U(z)]$, the web is run at a speed of 1.266 m/s (250 FPM), and a pseudorandom signal is used as the input for the dancer roller velocity. The dancer velocity input $U(k)$ and variations in tension in the span downstream to the dancer roller $T_2(k)$ are acquired at each sampling period. The Box-Jenkins model [16], given by the following equation, is used to represent the relation between $T_2(k)$ and $U(k)$:

$$\hat{G}(z) = \frac{T_2(z)}{U(z)} = \frac{-0.0173z^3 + 0.0359z^2 + 0.1257z - 0.1351}{z^{10} - 1.161z^9 - 0.9063z^8 + 0.8857z^7 + 0.9595z^6 - 0.2485z^5 - 0.9768z^4 + 0.1006z^3 + 0.7366z^2 - 0.3341z - 0.0557}. \quad (28)$$

The relative degree of the experimentally identified transfer function, Eq. (28), is much higher than the theoretical model, Eq. (22). This can be attributed to the fact that the dynamics of the motor, the platform containing the dancer roller, and of the load cell are not taken into account in the theoretical model. Since such high-order transfer functions are not amenable for analysis, model reduction technique using Bilinear Schwartz approximation [19] is used to obtain a lower-order approximation of $\hat{G}(z)$. The fourth-order Bilinear Schwartz approximation of Eq. (28) is

$$\hat{G}_4(z) = \frac{0.05462z^3 - 0.2269z^2 + 0.3071z - 0.1335}{z^4 - 3.103z^3 + 3.581z^2 - 1.773z + 0.2948}. \quad (29)$$

The Bode plots of the experimentally identified transfer function $\hat{G}(z)$, the reduced fourth-order model $\hat{G}_4(z)$, and the theoretical model are shown in Fig. 11. From the Bode plots, it can be observed that the reduced fourth-order model is very similar to the original tenth-order identified model. Further, it can also be observed that the behavior of the theoretical model is similar to that of the identified model, except for variations in the low-frequency gain and the corner frequency, in the frequency range of interest, which is up to 50 rad/s (8 Hz). Also, notice that the identified model has a pair of under damped poles around 80 rad/s (13 Hz) frequency region, which are not reflected in the theoretical model; these poles may reflect resonant conditions of the active dancer structure, load cells, or the experimental platform structure.

7 Implemented Controllers and Experimental Results

Three types of controllers were implemented for the active dancer system: a proportional-integral-derivative controller (PID),

$$T_2(k) = G(z^{-1})U(k) + H(z^{-1})e(k), \quad (27)$$

where

$$G(z^{-1}) = B(z^{-1})/F(z^{-1}),$$

$$H(z^{-1}) = C(z^{-1})/D(z^{-1}),$$

$$B(z^{-1}) = b_0 + b_1z^{-1} + \dots + b_{n_b}z^{-n_b},$$

$$F(z^{-1}) = 1 + f_1z^{-1} + \dots + f_{n_f}z^{-n_f},$$

$$C(z^{-1}) = 1 + c_1z^{-1} + \dots + c_{n_c}z^{-n_c},$$

$$D(z^{-1}) = 1 + d_1z^{-1} + \dots + d_{n_d}z^{-n_d},$$

$e(k)$ is white noise, and

z^{-1} represents the unit delay operator.

The term $H(z^{-1})e(k)$ is included to account for the terms T_0 , and T_3 in Eq. (22) and other disturbances affecting the tension T_2 . Using this model and the data obtained, generalized partial auto-correlation function (GPAC) technique [17] is used to estimate the orders of the polynomials $B(z^{-1})$, $F(z^{-1})$, $C(z^{-1})$, and $D(z^{-1})$; these orders are found to be $n_b = 3$, $n_f = 10$, $n_c = 1$, and $n_d = 1$. The coefficients, b_i , f_i , c_i , were estimated using the Levenberg-Marquardt algorithm [18]. The Appendix gives a step-by-step procedure of the identification technique used to arrive at the input-output model. The identified transfer function from the dancer roller velocity input to the downstream tension is

an internal model based controller (IMC), and a linear quadratic regulator (LQR). The internal model based controller consists of a proportional controller and an internal model of sinusoidal tension disturbance with a known frequency and unknown amplitude. The frequency of the tension disturbance is obtained by taking a fast-Fourier transform (FFT) of the tension signal obtained from the

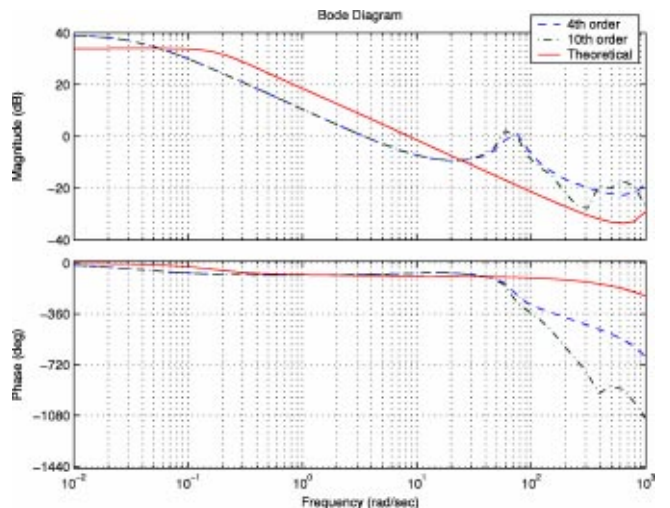


Fig. 11 Theoretical and identified Bode plots

load cell located upstream of the dancer roller. A description of the design of three controllers implemented is presented in the following.

The pulse transfer function of the PID controller that is experimentally implemented is

$$G_c(z) := \frac{U(z)}{T_2(z)} = K_p + \frac{K_i}{1-z^{-1}} + K_d(1-z^{-1}) = \frac{K_1 - K_2 z^{-1} + K_3 z^{-2}}{1-z^{-1}}, \quad (30)$$

where K_p , K_i , and K_d are proportional, integral, and derivative gains, respectively, and $K_1 = K_p + K_i + K_d$, $K_2 = K_p + 2K_d$, and $K_3 = K_d$. The gains K_1 , K_2 , and K_3 were chosen to place the closed-loop poles of the active dancer system with the following design requirements: percentage peak overshoot of less than 10% and the settling time of less than 1 s. This design process was carried out using the “rltool” utility in MATLAB. The following gain values were obtained: $K_p = 1.932$, $K_d = 0.8063$, and $K_i = 2.1099$. Figure 12 shows the performance of the PID controller; the top two plots correspond to the measured periodic tension disturbance and its FFT, and the bottom two plots show the measured tension error and its FFT when the active dancer roller is under PID control. Notice that the frequency of tension disturbance is about 25.13 rad/s (4 Hz) when the line is running at a reference speed of 1.772 m/s (350 FPM).

In the internal model based type of controller, a proportional controller is augmented with an internal model of the disturbance; the classical internal model principle is used. The disturbance frequency, ϑ , is measured by taking an FFT of the measured ten-

sion signal from the load cell prior to implementing the controller. The following is the structure of the IMC controller that was implemented:

$$G_c(z) = \frac{K_p + z^{-1} K_{imc} \sin(\vartheta T_s)}{1 - 2z^{-1} \cos(\vartheta T_s) + z^{-2}}, \quad (31)$$

where K_p is the proportional gain, T_s is the sampling period, and K_{imc} is the tunable gain to compensate for the unknown amplitude of the periodic tension disturbance. Using the “rltool” utility of MATLAB, the gains K_p and K_{imc} were calculated for each of the web speeds to place the closed-loop poles such that the settling time is less than 1 s and percentage overshoot is less than 10%. The following gains were obtained and used in the experiments: $K_p = 0.04607$ and $K_{imc} = 0.04607$.

In the experimental platform shown in Fig. 9, tension disturbance is created by an out-of-round roller in the web path. Thus, the disturbance frequency is proportional to the web speed. Experiments were conducted at various web speeds (thus, different known disturbance frequencies) and a representative result is shown in Fig. 13; this also corresponds to a line speed of 1.772 m/s (350 FPM) which results in a disturbance frequency of about 25.13 rad/s (4 Hz). The top two plots of Fig. 13 show the controlled tension with IMC controller and the FFT of the controlled tension, respectively.

To formulate a traditional stationary LQR problem for the active dancer system, we consider the state space equations obtained from the input-output model given by Eq. (26). The state space equations can be expressed in the matrix form as

$$\begin{aligned} \xi(k+1) &= G\xi(k) + H_u U(k), \\ y(k) &= C\xi(k). \end{aligned} \quad (32)$$

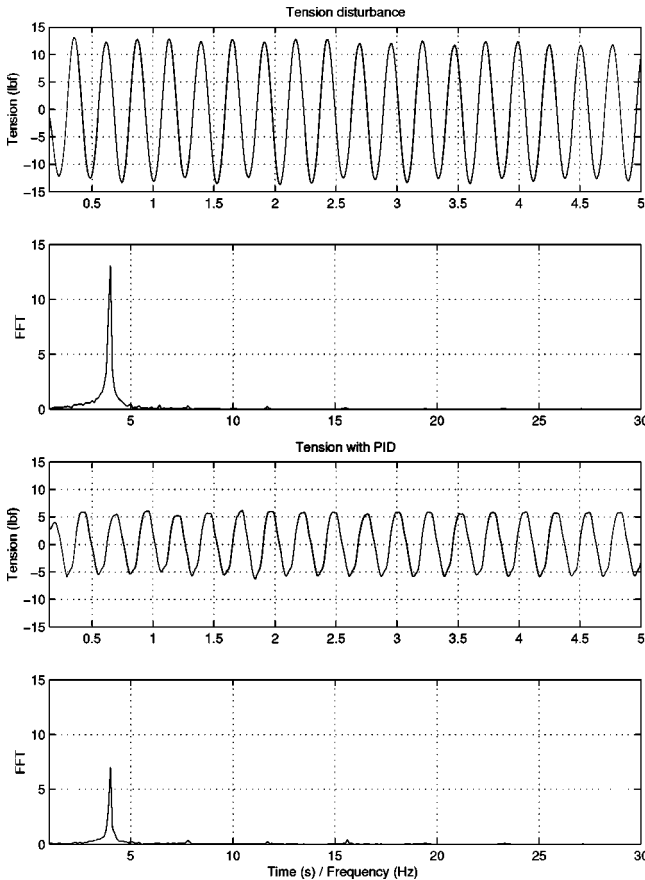


Fig. 12 Tension with out-of-round idle roller (disturbance and PID control); $v_r = 1.772$ m/s (350 FPM), $t_r = 160.14$ N (36 lbf)

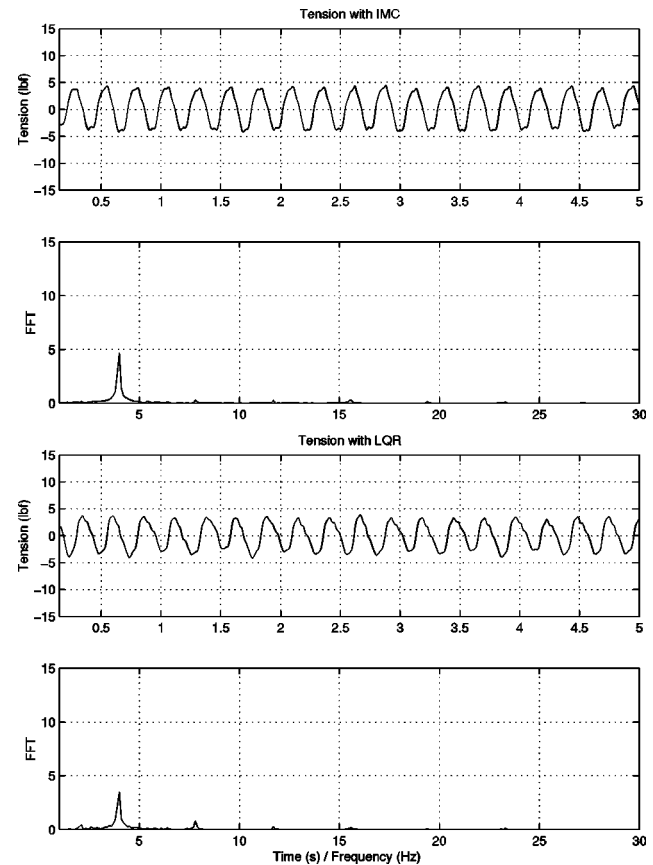


Fig. 13 Tension with out-of-round idle roller (IMC and LQR); $v_r = 1.772$ m/s (350 FPM), $t_r = 160.14$ N (36 lbf)

The following performance index is used to obtain the optimal control input:

$$J = \frac{1}{2} \sum_{k=0}^{\infty} [y^2(k) + R_{lqr} U^2(k)], \quad (33)$$

where R_{lqr} is the weighting factor that penalizes control input magnitude. The control input that results from minimizing the above performance index is a state feedback controller of the form $U(k) = -K\xi(k)$. A Luenberger observer was used to estimate the state variables based on the measured tension. A control weighting factor value of 0.1, i.e., $R_{lqr} = 0.1$, was used; any value smaller than this resulted in the control effort being very large and exceeding the active dancer motor velocity limits. The control and observer gain vectors that were computed off-line and used in the experiments were $K = 10^{-3}(0.0011306, 0.77836, 53.584, 207.95)$ and $L = (-0.96586, 3.8969, -5.8833, 3.773)$, respectively.

Experiments were conducted at various web speeds and a representative result for the reference web speed of 1.772 m/s (350 FPM) for the LQR controller is shown in the bottom two plots of Fig. 13; the bottom two plots show the controlled tension with LQR controller and the FFT of the controlled tension, respectively.

A summary of the amount of tension disturbance magnitude reduction for PID, IMC, and LQR controllers for four different web speeds, 1.013 m/s, 1.266 m/s, 1.519 m/s, 1.772 m/s (200 FPM, 250 FPM, 300 FPM, and 350 FPM) is shown in Fig. 14. The summary shown in Fig. 14 indicates that all the three controllers give good attenuation of the periodic tension disturbance using the active dancer. Notice that at the low speed of 1.012 m/s (200 FPM), the attenuation level of all three controllers is similar but as the speed is increased the attenuation level is more for the IMC and the LQR controllers. It is not clear from a number of experiments as to why there is a variation of tension attenuation levels at different speeds, and why the tension attenuation level drops from 1.266 to 1.519 m/s whereas it increases from 1.519 to 1.772 m/s. We believe that one possible reason for this could be due to the endless web line that is used in the experiments; in an endless web line the same web loops around in the platform. We have assumed that there is no propagation of tension in the upstream direction from the web span where tension disturbances are created; this is true only when there is not slip on the rollers. We plan to investigate this further after incorporating unwind/rewind stands into the current experimental platform.

Experimental results show that the active dancer system is effective in attenuating periodic tension disturbances. The distur-

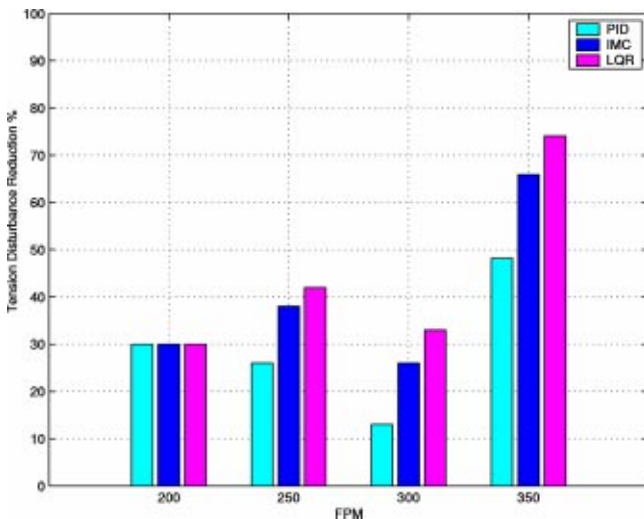


Fig. 14 Summary of tension disturbance reduction

bance rejection capability of the active dancer system is limited only by the bandwidth limitation of the actuator as opposed to the passive dancer or an inertia compensated dancer which are known to have considerable resonance problems.

8 Conclusions and Future Work

In this paper, a mathematical model of an active dancer system which can be used for periodic tension disturbance attenuation has been developed. An experimental web platform with an active dancer system has been developed to conduct real-time experiments. Data collected from an extensive set of experiments validate the usefulness of an active dancer in attenuation of periodic web tension disturbance in a web process line. Further, analysis of the model reveals a structural limitation on the design of the active dancer system, which is the ratio of the downstream to upstream web span length with respect to the active dancer roller must be less than 2 for tension attenuation using an active dancer.

Future research will focus on incorporating the active dancer mechanism in an unwind/rewind web process line. This work assumed that there is no slip of the web on the dancer roller, which may not be the case at high web speeds and large amplitude periodic tension disturbances. Our future work will also focus on the study of slip on the dancer roller. In this paper, we have investigated the effectiveness of the active dancers for steady operating speeds and tensions, that is, we have considered the linearized system. Future work will include design of the controllers, such as iterative learning controllers [20,21] and robust adaptive controllers, for the complete nonlinear model that accounts for transients during startup and shutdown conditions in web process lines.

Acknowledgments

The authors acknowledge the support of the Web Handling Research Center, the Oklahoma Center for Advancement of Science and Technology under Project No. AR982-021, and the National Science Foundation under Grant No. CMS 9982071.

Nomenclature

- A = Cross-sectional area of web
- B_f = Bearing friction
- E = Modulus of elasticity
- J = Polar moment of inertia of roller
- R = Radius of a roller
- v_r = Reference web velocity
- t_r = Reference web tension
- τ = Time
- L_i = Length of the i th web span
- t_i = Tension in the i th web span
- v_i = Web velocity on the i th roller
- T_i = Change in tension from the reference
- V_i = Change in web velocity from the reference
- τ_i = Time constant of a web span (L_i/v_r)
- K_i = Web span spring constant (EA/L_i)
- X = Change in linear displacement of the dancer roll from the reference
- U = Dancer translational velocity input
- $\alpha, \beta, \gamma, \eta$ = System constants ($EA/v_r, J/R^2, B_f/R^2, \beta/\alpha$)
- ε_i = Strain in the i th web span
- ε_{iv} = Strain due to velocity variation in the i th web span
- ε_{id} = Strain due to dancer displacement in the i th web span (applies only to spans next to the dancer roll)
- θ_1, θ_2 = Wrap angles on upstream and downstream side of dancer roll

Appendix: Identification Procedure

The dynamics between the tension t_2 and the dancer velocity u is described in the form of the Box-Jenkins Model as

$$T_2(k) = G(z^{-1})U(k) + H(z^{-1})e(k). \quad (34)$$

To estimate the transfer function we go through the following steps: (1) Estimate the impulse response for $G(z)$, (2) Find the orders of the numerator and denominator in the transfer function $G(z)$, and (3) Estimate the coefficients in the numerator and the denominator polynomials.

To estimate the impulse response, $\hat{g}(k)$, of the transfer function $G(z)$, assume that the input $u(k)$ and the white noise $e(k)$ are not correlated and $\hat{g}(k)=0$ for some $k>K$, then

$$y(t) = \sum_{i=0}^K \hat{g}(i)u(t-i). \quad (35)$$

Multiplying both sides of Eq. (35) by $u(t-k)$ and taking expectation and simplifying yields

$$R_{uy}(k) = \sum_{i=0}^K \hat{g}(i)R_u(k-i), \quad k=0,1,2,\dots,K. \quad (36)$$

$$\phi_{kk}^j = \frac{\begin{vmatrix} \hat{g}(j-1) & \hat{g}(j-2) & \cdots & \hat{g}(j-k+1) & \hat{g}(j) \\ \hat{g}(j) & \hat{g}(j-1) & \cdots & \hat{g}(j-k+2) & \hat{g}(j+1) \\ \vdots & \vdots & \vdots & \vdots & \vdots \\ \hat{g}(j+k-2) & \hat{g}(j+k-3) & \cdots & \hat{g}(j-2) & \hat{g}(j+k-1) \end{vmatrix}}{\begin{vmatrix} \hat{g}(j-1) & \hat{g}(j-2) & \cdots & \hat{g}(j-k+1) & \hat{g}(j-k) \\ \hat{g}(j) & \hat{g}(j-1) & \cdots & \hat{g}(j-k+2) & \hat{g}(j-k+1) \\ \vdots & \vdots & \vdots & \vdots & \vdots \\ \hat{g}(j+k-2) & \hat{g}(j+k-3) & \cdots & \hat{g}(j-2) & \hat{g}(j-1) \end{vmatrix}}. \quad (38)$$

As shown in Ref. [21], the GPAC function has the property that $\phi_{kk}^{n_b}=0$ for $k=n_f+1, n_f+2, \dots$, and ϕ_{kk}^j is of the form 0/0 for $j=n_b+1, n_b+2, \dots$, and $k=n_f+1, n_f+2, \dots$. This property can be used to identify the orders of the numerator and the denominator polynomials of the transfer function. In a similar way, we can find the orders of the numerator and the denominator, n_c and n_d , of the transfer function $H(z)$.

Once the orders of the numerator and the denominator of the transfer function are known, the Levenberg-Marquardt algorithm was used to estimate the unknown coefficients, b_0, b_1, \dots, b_{n_b} , f_1, f_2, \dots, f_{n_f} , c_1, c_2, \dots, c_{n_c} , and d_1, d_2, \dots, d_{n_d} . To this end, define the estimate of the parameter vector in the k th iteration as

$$\hat{\psi}_k = [\hat{b}_0, \dots, \hat{b}_{n_b}, \hat{f}_1, \dots, \hat{f}_{n_f}, \hat{c}_1, \dots, \hat{c}_{n_c}, \hat{d}_1, \dots, \hat{d}_{n_d}]^T. \quad (39)$$

The estimated output and residue of estimation can be computed as

$$\hat{y}(t|\hat{\psi}_k) = \hat{H}^{-1} \hat{G}(q)u(t) + [1 - \hat{H}^{-1}]y(t), \quad (40)$$

$$\varepsilon(\hat{\psi}_k) = y(t) - \hat{y}(t|\hat{\psi}_k).$$

Now, we consider the cost function defined by $F(\hat{\psi}_k) = \sum_{t=1}^N \varepsilon^T(\hat{\psi}_k)\varepsilon(\hat{\psi}_k)$ where N is the total number of data points, can be considered for minimization. The Levenberg-Marquardt algorithm uses a gradient search method which requires the computation of the vector $J(\hat{\psi}_k)$ defined as

$$J(\hat{\psi}_k) = - \left[\frac{\partial \hat{y}(t|\hat{\psi}_k)}{\partial \hat{\psi}_k(1)} \quad \frac{\partial \hat{y}(t|\hat{\psi}_k)}{\partial \hat{\psi}_k(2)} \quad \cdots \quad \frac{\partial \hat{y}(t|\hat{\psi}_k)}{\partial \hat{\psi}_k(n)} \right], \quad (41)$$

where n is the total number of parameters to be estimated. Each element in this vector can be computed numerically. The algo-

The above equations can be written in matrix form as

$$\begin{bmatrix} R_u(0) & R_u(1) & \cdots & R_u(K) \\ R_u(1) & R_u(0) & \cdots & R_u(K-1) \\ \vdots & \vdots & \vdots & \vdots \\ R_u(K) & R_u(K-1) & \cdots & R_u(0) \end{bmatrix} \begin{bmatrix} \hat{g}(0) \\ \hat{g}(1) \\ \vdots \\ \hat{g}(K) \end{bmatrix} = \begin{bmatrix} R_{uy}(0) \\ R_{uy}(1) \\ \vdots \\ R_{uy}(K) \end{bmatrix}. \quad (37)$$

From Eq. (37) $\hat{g}(i)$ for $i=0,1,\dots,K$, can be computed. In the experiments K was chosen to be 50.

To find the orders of the numerator and the denominator polynomials (n_b and n_f) of the transfer function $G(z)$, the generalized partial autocorrelation (GPAC) function method as given in Refs. [17], [21] is used. The GPAC function ϕ_{kk}^j is defined as

gorithm terminates when a tolerance specified by $J \text{grad}_{\min}$ is met. This algorithm also requires an initial value μ_0 of μ and a multiplier (divisor) ν to account for fast (slow) convergence. The Levenberg-Marquardt algorithm is

- (1) Input ψ_0 , minimal gradient $J \text{grad}_{\min}$, μ_0 , ν , $u(t)$, and $y(t)$.
- (2) Repeat the following starting with $k=0$.
- (3) Set $k=k+1$ and $\mu_{k+1} = \mu_k / \nu$.
- (4) Compute $J(\hat{\psi}_k)$, $\varepsilon(\hat{\psi}_k)$.
- (5) Solve for $\Delta \hat{\psi}_k$ from $[J^T(\hat{\psi}_k)J(\hat{\psi}_k) + \mu_k I] \Delta \hat{\psi}_k = -J^T(\hat{\psi}_k)\varepsilon(\hat{\psi}_k)$.
- (6) Update the parameter vector $\hat{\psi}_{k+1} = \hat{\psi}_k + \Delta \hat{\psi}_k$.
- (7) If $F(\hat{\psi}_{k+1}) \geq F(\hat{\psi}_k)$, set $\mu_k = \mu_k * \nu$ and go to step 5. Otherwise continue.
- (8) Set $\mu_{k+1} = \mu_k$.
- (9) If $\|2J^T(\hat{\psi}_{k+1})\varepsilon(\hat{\psi}_{k+1})\| < J \text{grad}_{\min}$ or $\mu_k > \mu_{\max}$, terminate the computation. Otherwise go to step 3.

Complete details of the Levenberg-Marquardt algorithm can be found in Ref. [18].

References

- [1] Campbell, D. P., 1958, *Dynamic Behavior of the Production Process*, Process Dynamics, John Wiley and Sons, Inc., New York, first edition.
- [2] Grenfell, K. P., 1963, "Tension Control on Paper-Making and Converting Machinery," *IEEE 9-th Annual Conference on Electrical Engineering in the Pulp and Paper Industry*, Boston, MA, pp. 20-21.
- [3] King, D., 1969, "The Mathematical Model of a Newspaper Press," *Newspaper Techniques*, pp. 3-7.
- [4] Brandenburg, G., 1977, "New Mathematical Models for Web Tension and Register Error," *International IFAC Conference on Instrumentation and Automation in the Paper, Rubber, and Plastics Industry*, Vol. 1, pp. 411-438.
- [5] Shelton, J. J., 1986, "Dynamics of Web Tension Control With Velocity or Torque Control," *Proceedings of the American Control Conference*, Seattle, WA, pp. 1423-1427.
- [6] Shin, K. H., 1991, "Distributed Control of Tension in Multi-Span Web Transport Systems," Ph.D. thesis, Oklahoma State University, Stillwater, Oklahoma.

- [7] Young, G. E., and Reid, K. N., 1993, "Lateral and Longitudinal Dynamic Behavior and Control of Moving Webs," *ASME J. Dyn. Syst., Meas., Control*, **115**, pp. 309–317.
- [8] Wolfermann, W., 1995, "Tension Control of Webs, a Review of the Problems and Solutions in the Present and Future," *Proceedings of the Third International Conference on Web Handling*, pp. 198–229.
- [9] Shelton, J. J., 1999, "Limitations to Sensing of Web Tension by Means of Roller Reaction Forces," *Proceedings of the Fifth International Conference on Web Handling*.
- [10] Reid, K. N., and Lin, K. C., 1993, "Dynamic Behavior of Dancer Subsystems in Web Transport Systems," *Proceedings of the Second International Conference on Web Handling*, pp. 135–146.
- [11] Kuribayashi, K., and Nakajima, K., 1984, "An Active Dancer Roller System for Tension Control of Wire and Sheet," *Proceedings of the 9th Triennial World Congress of IFAC*, Budapest, Hungary, pp. 1747–1752.
- [12] Rajala, G. J., 1995, Active Dancer Control for Web Handling Machine, M.S. thesis, University of Wisconsin, Madison, WI.
- [13] Pagilla, P. R., Perera, L. P., and Dwivedula, R. V., 2001, "The Role of Active Dancers in Tension Control of Webs," *Proceedings of the Sixth International Conference on Web Handling*.
- [14] Perera, L. P., 2001, "The Role of Active Dancers in Tension Control of Webs," M.S. thesis, Oklahoma State University, Stillwater, OK.
- [15] Skogestad, S., and Postlethwaite, I., 1996, *Multivariable Feedback Control: Analysis and Design*, John Wiley and Sons, New York.
- [16] Ljung, L., and Soderstrom, T., 1983, *Theory and Practice of Recursive Identification*, MIT Press, Cambridge, MA.
- [17] Woodward, W. A., and Gray, H. L., 1981, "On the Relationship Between the S Array and the Box-Jenkins Method of ARMA Model Identification," *J. Am. Stat. Assoc.*, **76**, pp. 579–587.
- [18] Hagan, M., Demuth, H., and Beale, M., 1996, *Neural Network Design*, PWS Publishing, Boston, MA.
- [19] Hsieh, C.-H., and Hwang, C., 1990, "Model Reduction of Linear Discrete-Time Systems Using Bilinear Schwarz Approximation," *Int. J. Syst. Sci.*, **21**, pp. 33–49.
- [20] Moore, K. L., Dahleh, M., and Bhattacharya, S. P., 1992, "Iterative Learning Control: A Survey and New Results," *J. Rob. Syst.*, **9**, pp. 563–594.
- [21] Abdul-AI-Nadi, D. I., 1991, ARMA Order Determination, M.S. thesis, Oklahoma State University.